

Anisotropic magnetoresistance and upper critical fields up to 63 T in $\text{CaKFe}_4\text{As}_4$ single crystals

Tai Kong,¹ Fedor F. Balakirev,² William R. Meier,¹ Sergey L. Bud'ko,¹ Alex Gurevich,³ and Paul C. Canfield¹

¹*Ames Laboratory, U.S. DOE, and Department of Physics and Astronomy, Iowa State University, Ames, Iowa 50011, USA*

²*National High Magnetic Field Laboratory, Los Alamos National Laboratory, MS-E536, Los Alamos, New Mexico 87545, USA*

³*Department of Physics, Old Dominion University, Norfolk, Virginia 23529, USA*

We report the temperature dependencies of the upper critical fields $H_{c2}^c(T)$ parallel to the c-axis and $H_{c2}^{ab}(T)$ parallel to the ab-plane of single crystalline $\text{CaKFe}_4\text{As}_4$ inferred from the measurements of the temperature-dependent resistance in static magnetic fields up to 14 T and magnetoresistance in pulsed fields up to 63 T. We show that the observed decrease of the anisotropy parameter $\gamma(T) = H_{c2}^{ab}/H_{c2}^c$ from $\simeq 2.5$ at T_c to $\simeq 1.5$ at 25 K can be explained by interplay of paramagnetic pairbreaking and orbital effects in a multiband theory of H_{c2} . The slopes of $dH_{c2}^c/dT \simeq -4.4$ T/K and $dH_{c2}^{ab}/dT \simeq -10.9$ T/K at T_c yield an electron mass anisotropy of $m_{ab}/m_c \simeq 1/6$ and short coherence lengths $\xi_c \simeq 5.8$ Å and $\xi_{ab} \simeq 14.3$ Å. The behavior of $H_{c2}(T)$ turns out to be similar to that of the optimal doped $(\text{Ba,K})\text{Fe}_2\text{As}_2$, with $H_{c2}^{ab}(0)$ extrapolating to $\simeq 92$ T, well above the BCS paramagnetic limit.

The discovery of Fe-based superconductors (FBS)¹ has intensified research on mechanisms of high-temperature-superconductivity and searches for materials with higher superconducting transition temperatures T_c . Among the many different classes of FBS², the so called "122" family with a ThCr_2Si_2 -type structure (I4/mmm) is one of the most well-studied systems. Superconductivity in the "122" family was first discovered in $(\text{Ba,K})\text{Fe}_2\text{As}_2$ ³ with alkali metal (A) /alkali earth (Ae) substitution. Subsequently it was found that superconductivity can also be induced by transition metal substitutions⁴⁻⁶ or substitutions on the As site⁷. In these substitution cases, though, the ThCr_2Si_2 -type structure remained the same. However, when the difference in ionic radii between the A and Ae ions becomes larger, such as in the case of Ca and K, a homogeneous substitution on the A/Ae site could not be reached⁸.

Recently, Iyo et al.⁹ systematically studied the structure of (A,Ae) Fe_2As_2 polycrystals and stabilized a new $\text{AeAFe}_4\text{As}_4$ structure type (P4/mmm) with alternating A/Ae layers separated by Fe-As layers when the A/Ae ionic radii are sufficiently different. Unlike a homogeneous substitution within the ThCr_2Si_2 -type structure, each A/Ae in the $\text{AeAFe}_4\text{As}_4$ structure occupies a unique, well-defined, crystallographic site. Single crystals of $\text{CaKFe}_4\text{As}_4$ were synthesized and characterized soon after the initial discovery¹⁰. $\text{CaKFe}_4\text{As}_4$ is found to be superconducting at ~ 35 K with no other phase transitions from 1.8 K to 300 K¹⁰. The pressure dependence of T_c , anisotropic electric resistivity, elastoresistivity, Hall effect and thermal power data suggest that $\text{CaKFe}_4\text{As}_4$ behaves similarly to optimal, or slightly overdoped, $(\text{Ba,K})\text{Fe}_2\text{As}_2$ ¹⁰. Anisotropic $H_{c2}(T)$ data were measured up to 14 T; over this very limited field and temperature range, the anisotropic $H_{c2}(T)$ curves for $\text{CaKFe}_4\text{As}_4$ look a lot like those of $\text{Ba}_{0.55}\text{K}_{0.45}\text{Fe}_2\text{As}_2$ ¹¹. But, clearly, significantly higher field data will be necessary to reveal H_{c2} at low temperatures.

The newly discovered $\text{CaKFe}_4\text{As}_4$ is expected to have

very high upper critical fields $H_{c2}(T)$ mediated by the characteristic of FBS interplay of multiband orbital effects and strong Pauli pairbreaking^{12,13}. Yet the extent to which the above features of $\text{CaKFe}_4\text{As}_4$ can manifest themselves in the high-field behavior of $H_{c2}(T)$ and whether it would be different from that of the well-studied 122 FBS^{14,15} has not yet been addressed. Another intriguing question is whether multiband superconductivity in ordered $\text{CaKFe}_4\text{As}_4$ could result in crossing of the upper critical field curves $H_{c2}^c(T)$ parallel to the c-axis and $H_{c2}^{ab}(T)$ parallel to ab-plane, as has been observed in some FBS and other superconductors¹⁶⁻¹⁸. The anticipated lack of the effect of disorder on multiband superconductivity in $\text{CaKFe}_4\text{As}_4$ also makes this material (along with other such stoichiometric FBS as LiFeAs ¹⁹) a good candidate for searching for the Fulde-Ferrel-Larkin-Ovchinnikov (FFLO) states^{12,13,20-22}. To address these points, in this paper we present measurements of anisotropic magnetoresistance and $H_{c2}(T)$ in $\text{CaKFe}_4\text{As}_4$ single crystals in high magnetic fields up to 63 T.

Samples were grown using a high-temperature solution growth technique out of excess FeAs. Elemental K (Alfa Aesar, 99.95%), Ca (Ames Lab, 99.9+%) and pre-reacted FeAs (Fe: Alfa Aesar, 99.9+%. As: Alfa Aesar, 99.9999%) with a starting molar ratio of Ca:K:FeAs = 0.8:1.2:10 were held in an alumina frit-disc crucible set²³ and sealed in Ta tube, which were then sealed in a silica jacket under partial Ar atmosphere²⁴. Slightly more K than Ca was used to suppress the formation of CaFe_2As_2 . The packed ampoule was then heated up to 1180 °C, held at 1180 °C for 5 hours, rapidly cooled to 1050 °C and then slowly cooled to 930 °C, at which temperature the single crystals and the liquid was separated in a centrifuge. Single crystals are plate-like with typical dimension of $5 \times 5 \times 0.1$ mm. More detailed growth procedures can be found in Ref. 10.

The upper critical field $H_{c2}(T)$ was inferred from transport magnetoresistance measured by a standard four-

probe technique. Both DuPont 4929N silver paint and Epotek-H20E silver epoxy were used to attach contact leads onto the samples (Pt for measurements static field measurements and twisted copper wires for pulsed field measurements). For static fields below 14 T, resistance was measured using a Quantum Design (QD) physical property measurement system, PPMS-14 ($T = 1.8\text{--}305$ K, $H = 0\text{--}14$ T, $f = 17$ Hz.). Higher field data were obtained in a 63 T pulsed magnet at the National High Magnetic Field Laboratory (NHMFL), Los Alamos, using a high-frequency, synchronous digital lock-in technique ($f = 148$ kHz).

Fig. 1 shows the temperature-dependent resistance measured at different applied fields in a QD PPMS. The criteria for determining T_c are shown in Fig. 1(a). The onset criterion identifies the temperature at which the normal state line intersects with the maximum slope of the resistance curve. The offset criterion identifies the temperature of the intersection of the maximum slope of the resistance curve and the zero-resistance line. In zero field, the superconducting transition is very sharp. As field is increased, the transition becomes slightly broader, more so for $H \parallel c$ than for $H \parallel ab$. For $H \parallel c$, the T_c value is suppressed to a lower temperature than for $H \parallel ab$ at a given field.

Fig. 2 shows the field-dependent resistance measured at different temperatures. A temperature-independent background was subtracted from the signal for clarity. The background is attributed to the displacement of the sample and its wiring by Lorentz force synchronous with lock-in excitation current. The resulting magnetic induction voltage is a product of field intensity and Lorentz force, leading to a stray background signal proportional to H^2 . Similar onset and offset criteria were applied to extract the superconducting field values at a given temperature. For $H \parallel c$ at 15 K, only an offset value could be resolved as shown in Fig. 2(a).

The anisotropic $H_{c2}(T)$ data inferred from the temperature-dependent and field-dependent resistance data, summarized in Fig. 3, reveal multiple features about $\text{CaKFe}_4\text{As}_4$. (1) The values of $H_{c2}(0)$ both parallel and perpendicular to the c -axis extrapolate to the fields well above the single-band BCS paramagnetic limit $H_p[T] = 1.84T_c[K] \simeq 64$ T, which is close to the maximum field in our pulse magnet. Thus, Pauli pair-breaking is essential, similar to the majority of other FBS¹³. (2) As a result of different temperature dependencies of $H_{c2}^c(T)$ and $H_{c2}^{ab}(T)$ the anisotropy parameter $\gamma(T) = H_{c2}^{ab}(T)/H_{c2}^c(T)$ decreases as T decreases (see upper inset in Fig. 3), consistent with the interplay of orbital and Pauli pairbreaking¹². (3) No crossing of $H_{c2}^c(T)$ and $H_{c2}^{ab}(T)$ was observed at $0 < H < 61$ T, although a possibility that it may happen at higher fields cannot be ruled out.

The superconducting coherence lengths $\xi_{ab}(T) = \xi_{ab}\tau^{-1/2}$ in the ab plane and $\xi_c(T) = \xi_c\tau^{-1/2}$ along the c -axis, as well as the electron band mass anisotropy can be estimated from the measured slopes of $dH_{c2}^c/dT \approx -4.4$

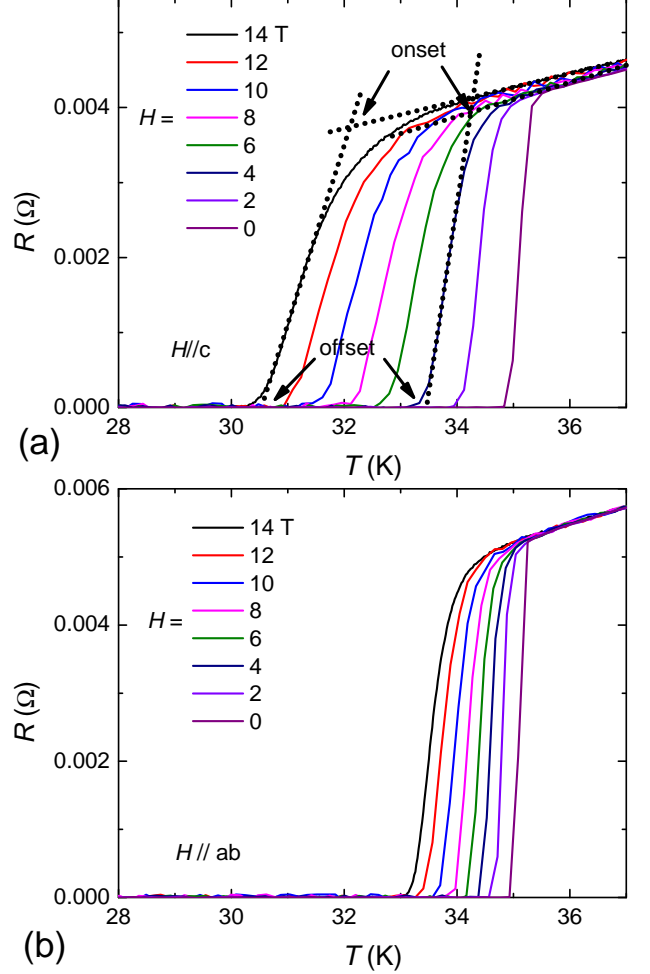


FIG. 1. (Color online) Temperature-dependent resistance measured in a QD PPMS at different applied fields with (a) $H \parallel c$ and (b) $H \parallel ab$. Dotted line and arrows indicate different criteria for determining H_{c2} (see text).

T/K and $dH_{c2}^{ab}/dT \approx -10.9$ T/K at T_c using the single-band Ginzburg-Landau (GL) theory, where $\tau = 1 - T/T_c$ [25]. From $|dH_{c2}^c/dT| = \phi_0/2\pi\xi_{ab}^2T_c$ and $|dH_{c2}^{ab}/dT| = \phi_0/2\pi\xi_{ab}\xi_cT_c$, where ϕ_0 is the magnetic flux quantum, we obtain $\xi_{ab} \simeq 14.3$ Å and $\xi_c \simeq 5.8$ Å. These coherence lengths are of the order of the lattice parameters⁹: $a = 3.866$ Å and $c = 12.817$ Å, the value ξ_c being half the unit cell height along the c -axis. The resulting electron effective mass anisotropy $\epsilon = m_{ab}/m_c = (\xi_c/\xi_{ab})^2 \simeq 1/6$ is similar to that of the 122 family of FBS and smaller than $m_c/m_{ab} \simeq 20 - 30$ characteristic of the 1111 FBS and $\text{YBa}_2\text{Cu}_3\text{O}_{7-x}$ ^{12,13}. Such short coherence lengths and the lack of structural disorder also suggest that $\text{CaKFe}_4\text{As}_4$ is in the clean limit as the mean free path $\ell \gg \xi_{ab}$ for the measured resistivity $\rho_n \sim 100 \mu\Omega \text{ cm}$.

To gain further insight into the behavior of $H_{c2}(T)$, we fitted the experimental data using a two-band theory which takes into account both orbital and Pauli pair-

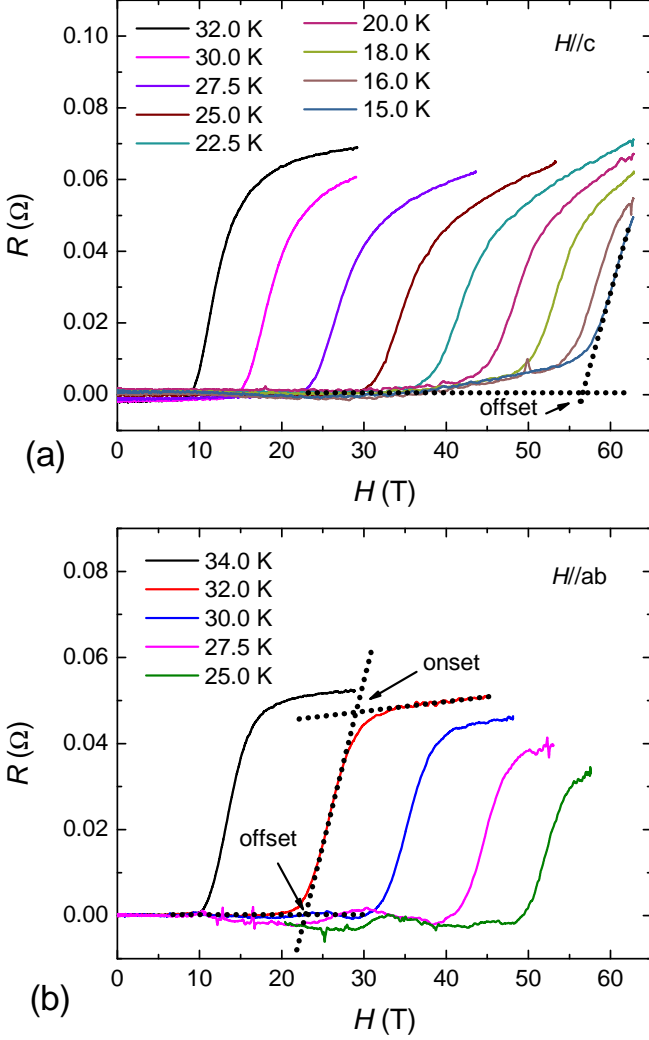


FIG. 2. (Color online) Field-dependent resistance measured in a 63 T pulsed magnet at different temperatures with (a) $H \parallel c$ and (b) $H \parallel ab$. A temperature-independent background signal was subtracted for clarity (see text). Dotted line and arrows indicate different criteria for determining H_{c2} (see text).

breaking in the clean limit for two ellipsoidal Fermi surfaces. In this case the equation for H_{c2}^c is given by^{12,13},

$$a_1 G_1 + a_2 G_2 + G_1 G_2 = 0, \quad (1)$$

$$G_1 = \ln t + 2e^{q^2} \operatorname{Re} \sum_{n=0}^{\infty} \int_q^{\infty} du e^{-u^2} \times \left[\frac{u}{n+1/2} - \frac{t}{\sqrt{b}} \tan^{-1} \left(\frac{u\sqrt{b}}{t(n+1/2) + i\alpha b} \right) \right]. \quad (2)$$

Here $a_1 = (\lambda_0 + \lambda_-)/2w$, $a_2 = (\lambda_0 - \lambda_-)/2w$, $\lambda_- = \lambda_{11} - \lambda_{22}$, $\lambda_0 = (\lambda_-^2 + 4\lambda_{12}\lambda_{21})^{1/2}$, $w = \lambda_{11}\lambda_{22} - \lambda_{12}\lambda_{21}$, $t = T/T_c$, λ_{11} and λ_{22} are the pairing constants in band 1 and 2, and λ_{12} and λ_{21} are interband pairing constants.

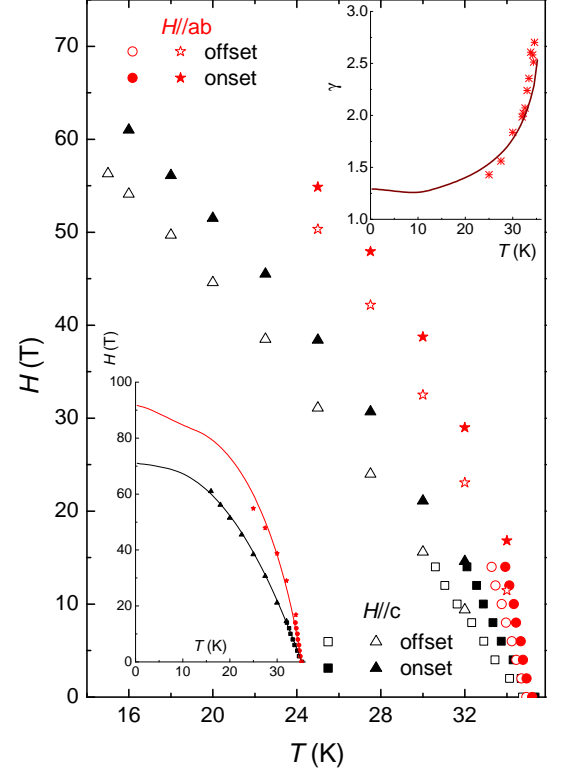


FIG. 3. (Color online) Anisotropic $H_{c2}(T)$ up to 61 T in $\text{CaKFe}_4\text{As}_4$ single crystals. Black squares (from PPMS) and black triangles (from pulsed magnet) represents $H_{c2}^c(T)$. Red circles (from PPMS) and red stars (from pulsed magnet) represents $H_{c2}^{\text{ab}}(T)$. Open and filled symbols indicate onset and offset criteria as described in the text. The upper inset shows the anisotropic parameter $\gamma(T) = H_{c2}^{\text{ab}}/H_{c2}^c$ together with the theoretically fitted curve (brown solid line). The lower inset shows the anisotropic $H_{c2}(T)$ data points from the onset criteria with the theoretically fitted curve (black and red solid lines). Previously, data measured by PPMS were presented in Ref.10.

The function G_2 is obtained by replacing $\sqrt{b} \rightarrow \sqrt{\eta b}$ and $q \rightarrow q\sqrt{s}$ in G_1 , where

$$b = \frac{\hbar^2 v_1^2 H_{c2}}{8\pi\phi_0 k_B^2 T_c^2}, \quad \alpha = \frac{4\mu\phi_0 k_B T_c}{\hbar^2 v_1^2}, \quad (3)$$

$$q^2 = Q^2\phi_0\epsilon_1/2\pi H_{c2}, \quad \eta = v_2^2/v_1^2, \quad s = \epsilon_2/\epsilon_1. \quad (4)$$

Here Q is the wave vector of the FFLO modulations of the order parameter, v_j is the in-plane Fermi velocity in band $j = 1, 2$, $\epsilon_j = m_j^{\text{ab}}/m_j^c$ is the mass anisotropy ratio, μ is the magnetic moment of a quasiparticle, $\alpha \approx 1.8\alpha_M$, and $\alpha_M = H_{c2}^{\text{orb}}/\sqrt{2}H_p$ is the Maki paramagnetic parameter. If \mathbf{H} is applied along the symmetry axis, \mathbf{Q} is parallel to \mathbf{H} and the magnitude of Q is determined by the condition $\partial H_{c2}/\partial Q = 0$ of maximum H_{c2} .

For the sake of simplicity, we consider here the case of $\epsilon_1 = \epsilon_2 = \epsilon$ for which the anisotropic H_{c2} can be written

in the scaling form

$$H_{c2}^c(T) = H_0 b(t, \eta, \alpha), \quad H_{c2}^{ab}(T) = \frac{H_0}{\sqrt{\epsilon}} b\left(t, \eta, \frac{\alpha}{\sqrt{\epsilon}}\right),$$

where $H_0 = 8\pi\phi_0 k_B^2 T_c^2 / \hbar^2 v_1^2$ and b is a solution of Eq. (1). The fit of the measured $H_{c2}(T)$ to Eq. (1) for s_{\pm} pairing with $\lambda_{11} = \lambda_{22} = 0$, $\lambda_{12}\lambda_{21} = 0.25$, $\eta = 0.2$, $\alpha = 0.5$, and $\epsilon = 1/6$ is shown in Fig. 3 where H_0 was adjusted to fit the magnitude of $H_{c2}^c(T)$. The value of α is consistent with those which have been used previously to describe $H_{c2}(T)$ of $\text{Ba}_{1-x}\text{K}_x\text{As}_2\text{Fe}_2$ ¹⁵.

The fit shows that the upper critical fields at $T = 0$ extrapolate to $H_{c2}^c(0) \approx 71$ T and $H_{c2}^{ab}(0) \approx 92$ T, the shape of $H_{c2}^c(T)$ being mostly determined by orbital effects moderately affected by the Pauli pairbreaking. By contrast, the shape of $H_{c2}^{ab}(T)$ is consistent with the essential Pauli pairbreaking in both bands, because of large respective Maki parameters $\alpha_1^{ab} = \alpha/\sqrt{\epsilon}$ and $\alpha_2^{ab} = \alpha/\eta\sqrt{\epsilon}$. In the available field range $0 < H < 61$ T where the H_{c2} data were obtained, the fit is not very sensitive to the particular values of the pairing constants and the band asymmetry parameter η , yet it suggests the FFLO state at $T < 13$ K and for higher fields H parallel to the ab planes. More definite conclusions about multi-band orbital effects and FFLO states could be made by analyzing low-temperature parts of the $H_{c2}^c(T)$ and $H_{c2}^{ab}(T)$, which would require even higher fields $H > 63$ T. This distinguishes $\text{CaKFe}_4\text{As}_4$ from other ordered stoichiometric FBS compounds like LiFeAs for which the entire anisotropic $H_{c2}(T)$ has been measured¹⁹.

Further insights into the magneto-transport behavior of $\text{CaKFe}_4\text{As}_4$ can be inferred from the fact that the resistance transition curves $R(T)$ shown in Figs. 1 and 2 broaden as H increases. This indicates an essential effect of thermal fluctuations of vortices similar to that has been extensively studied in high- T_c cuprates in which a superconductor at fields not far below $H_{c2}(T)$ is in a thermally-activated flux flow described by the ohmic resistivity²⁶:

$$\rho(T) = \rho_0 e^{-U(T,H)/k_B T}, \quad (5)$$

where $U(T, H) = U_0(1 - T/T_c)^\alpha (H_{c2}(0)/H)^\beta$ is the activation barrier, U_0 and the exponents α and β depend on details of pinning, and $\rho_0 \sim \rho_n$ ²⁶. If the offset temperature T_m in Fig. 1 is defined at a resistivity $\rho_m = \rho(T_m) \ll \rho_n$, it follows from Eq. (5) that the width of the resistive transition $T_c - T_m$ increases with H :

$$T_c - T_m \simeq T_c \left[\frac{k_B T_c}{U_0} \ln \frac{\rho_n}{\rho_m} \right]^{1/\alpha} \left[\frac{H}{H_{c2}(0)} \right]^{\alpha/\beta} \quad (6)$$

Broadening of the superconducting transition in $\text{CaKFe}_4\text{As}_4$ under magnetic field was also observed by measuring the step in the specific heat¹⁰.

At $H = 0$ thermal fluctuations can be quantified by the Ginzburg number $Gi = 0.5(2\pi\mu_0 k_B T_c \lambda_0^2 / \phi_0 \xi_c)^2$ expressed in terms of ξ_c and the London penetration depth

λ_0 at $H||c$ and $T = 0$. The values of λ_0 in $\text{CaKFe}_4\text{As}_4$ has not yet been measured, but for $\lambda_0 = 100 - 200$ nm characteristic of the majority of FBS, we obtain that $\text{CaKFe}_4\text{As}_4$ with $\xi_c = 0.6$ nm and $T_c = 35$ K, would have $Gi = 1.25 \cdot 10^{-4} - 2 \cdot 10^{-3}$, of the same order of magnitude as Gi for other FBS but smaller than $Gi \sim 10^{-2}$ for $\text{YBa}_2\text{Cu}_3\text{O}_{7-x}$ ^{27,28}. The offset point of $R(T, H) = 0$ in Fig. 1 can also be associated with the irreversibility field $H_p(T)$ of melting and thermal depinning of vortex structure. For instance, the melting field H_m of the ideal vortex lattice in a uniaxial superconductor at $H||c$ is defined by the equation $h_m/(1 - h_m)^3 = (1 - t)t_0^2/t^2$, where $h_m = H_m/H_{c2}$, $t_0 = \pi c_L^2/Gi^{1/2}$ and $c_L = 0.15 - 0.17$ is the Lindemann number²⁶. For weak thermal fluctuations, $H_{c2} - H_m \ll H_{c2}$, the above equation for h_m yields

$$H_{c2}(T) - H_m(T) \simeq H_{c2}(0) \left(\frac{Gi}{\pi^2 c_L^4} \right)^{1/3} \left(1 - \frac{T}{T_c} \right)^{2/3} \quad (7)$$

Taking $c_L = 0.17$ and $Gi = 10^{-4} - 10^{-3}$ in Eq. (7) gives $(Gi/\pi^2 c_L^4)^{1/3} \approx 0.23 - 0.5$, which shows that thermal fluctuations in $\text{CaKFe}_4\text{As}_4$ are not weak, as also characteristic of the majority of FBS which are intermediate between the conventional low- T_c superconductors in which vortex fluctuations are negligible and high- T_c cuprates in which the behavior of vortex matter at 77K is controlled by thermal fluctuations. Yet the width of the critical fluctuation region $T_c - T \lesssim Gi T_c \sim 0.04$ K even at $Gi = 10^{-3}$ is still significantly smaller than the observed width of the sharp resistive transition $\Delta T \simeq 0.4$ K at $H = 0$ shown in Fig. 1, as well as the width of the step in specific heat in zero field¹⁰. This suggests that, in addition to thermal fluctuations of the order parameter, the resistive transition at zero field can be broadened by extrinsic factors such as weak materials inhomogeneities in T_c . As H increases, the field-induced broadening becomes more pronounced, structural defects and inhomogeneities in T_c affecting both the thermally-activated flux flow resistance²⁶ and the vortex melting field²⁹.

In conclusion, our magneto-transport measurements of the temperature-dependent anisotropic $H_{c2}(T)$ of single crystalline $\text{CaKFe}_4\text{As}_4$ up to 63 T show that $H_{c2}(T)$ is controlled by interplay of orbital and paramagnetic effects which cause the anisotropy parameter $\gamma(T) = H_{c2}^{ab}(T)/H_{c2}^c(T)$ to decrease as the temperature decreases. Despite the fact that Ca and K occupy different sites in $\text{CaKFe}_4\text{As}_4$ as opposed to solid solutions in $(\text{Ba}, \text{K})\text{Fe}_2\text{As}_2$, the behavior $H_{c2}(T)$ turns out to be similar to that of the optimal doped $(\text{Ba}, \text{K})\text{Fe}_2\text{As}_2$ ^{11,15}. Measurements at lower temperature with higher fields will be needed to reveal more details about the physics of $\text{CaKFe}_4\text{As}_4$.

We would like to thank J. Betts, M. Jaime, R. McDonald, B. Ramshaw, M. Chan, U. Kaluarachchi, V. Taufour, R. Prozorov for useful discussions and experimental assistance. W.R.M. was funded by the Gordon and Betty Moore Foundation EPiQS Initiative through Grant GBMF4411. Work done at Ames Laboratory was sup-

ported by US Department of Energy, Basic Energy Sciences, Division of Materials Sciences and Engineering under Contract NO. DE-AC02-07CH11358. The NHMFL Pulsed Field Facility is supported by the National Science

Foundation, the Department of Energy, and the State of Florida through NSF Cooperative Grant No. DMR-1157490 and by U.S. DOE BES Science at 100T project.

- ¹ Y. Kamihara, T. Watanabe, M. Hirano, and H. Hosono, *J. Am. Chem. Soc.* **130**, 3296 (2008).
- ² G. R. Stewart, *Rev. Mod. Phys.* **83**, 1589 (2011).
- ³ M. Rotter, M. Tegel, and D. Johrendt, *Phys. Rev. Lett.* **101**, 107006 (2008).
- ⁴ A. S. Sefat, R. Jin, M. A. McGuire, B. C. Sales, D. J. Singh, and D. Mandrus, *Phys. Rev. Lett.* **101**, 117004 (2008).
- ⁵ N. Ni, M. E. Tillman, J.-Q. Yan, A. Kracher, S. T. Hannahs, S. L. Bud'ko, and P. C. Canfield, *Phys. Rev. B* **78**, 214515 (2008).
- ⁶ P. C. Canfield and S. L. Bud'ko, *Annu. Rev. Cond. Matt. Phys.* **1**, 27 (2010).
- ⁷ S. Jiang, H. Xing, G. Xuan, C. Wang, Z. Ren, C. Feng, J. Dai, Z. Xu, and G. Cao, *J. Phys.: Condens. Matter* **21**, 382203 (2009).
- ⁸ D. M. Wang, X. C. Shangguan, J. B. He, L. X. Zhao, Y. J. Long, P. P. Wang, and L. Wang, *J. Supercond. Nov. Magn.* **26**, 2121 (2013).
- ⁹ A. Iyo, K. Kawashima, T. Kinjo, T. Nishio, S. Ishida, H. Fujihisa, Y. Gotoh, K. Kihou, H. Eisaki, and Y. Yoshida, *J. Am. Chem. Soc.* **138**, 3410 (2016), pMID: 26943024.
- ¹⁰ W. R. Meier, T. Kong, U. S. Kaluarachchi, V. Taufour, N. H. Jo, G. Drachuck, A. E. Böhrer, S. M. Saunders, A. Sapkota, A. Kreyssig, M. A. Tanatar, R. Prozorov, A. I. Goldman, S. L. Bud'ko, and P. C. Canfield, *arXiv:1605.05617* (2016).
- ¹¹ M. M. Altarawneh, K. Collar, C. H. Mielke, N. Ni, S. L. Bud'ko, and P. C. Canfield, *Phys. Rev. B* **78**, 220505 (2008).
- ¹² A. Gurevich, *Phys. Rev. B* **82**, 184504 (2010).
- ¹³ A. Gurevich, *Rep. Prog. Phys.* **74**, 124501 (2011).
- ¹⁴ M. Kano, Y. Kohama, D. Graf, F. Balakirev, A. S. Sefat, M. A. McGuire, B. C. Sales, D. Mandrus, and S. W. Tozer, *J. Phys. Soc. Jpn.* **78**, 084719 (2009).
- ¹⁵ C. Tarantini, A. Gurevich, J. Jaroszynski, F. Balakirev, E. Bellingeri, I. Pallecchi, C. Ferdeghini, B. Shen, H. H. Wen, and D. C. Larbalestier, *Phys. Rev. B* **84**, 184522 (2011).
- ¹⁶ M. Fang, J. Yang, F. F. Balakirev, Y. Kohama, J. Singleton, B. Qian, Z. Q. Mao, H. Wang, and H. Q. Yuan, *Phys. Rev. B* **81**, 020509 (2010).
- ¹⁷ B. Maierov, P. Mele, S. A. Baily, M. Weigand, S.-Z. Lin, F. F. Balakirev, K. Matsumoto, H. Nagayoshi, S. Fujita, Y. Yoshida, Y. Ichino, T. Kiss, A. Ichinose, M. Mukaida, and L. Civale, *Supercond. Sci. Technol.* **27**, 044005 (2014).
- ¹⁸ F. F. Balakirev, T. Kong, M. Jaime, R. D. McDonald, C. H. Mielke, A. Gurevich, P. C. Canfield, and S. L. Bud'ko, *Phys. Rev. B* **91**, 220505 (2015).
- ¹⁹ K. Cho, H. Kim, M. A. Tanatar, Y. J. Song, Y. S. Kwon, W. A. Coniglio, C. C. Agosta, A. Gurevich, and R. Prozorov, *Phys. Rev. B* **83**, 060502 (2011).
- ²⁰ Y. Matsuda and H. Shimahara, *J. Phys. Soc. Jpn.* **76**, 051005 (2007).
- ²¹ A. G. Lebed, *Phys. Rev. Lett.* **107**, 087004 (2011).
- ²² M. D. Croitoru, M. Houzet, and A. I. Buzdin, *Phys. Rev. Lett.* **108**, 207005 (2012).
- ²³ P. C. Canfield, T. Kong, U. S. Kaluarachchi, and N. H. Jo, *Philos. Mag.* **96**, 84 (2016).
- ²⁴ T. Kong, S. L. Bud'ko, and P. C. Canfield, *Phys. Rev. B* **91**, 020507 (2015).
- ²⁵ M. Tinkham, *Introduction to Superconductivity* (Courier Dover Publications, 2012).
- ²⁶ G. Blatter, M. V. Feigel'man, V. B. Geshkenbein, A. I. Larkin, and V. M. Vinokur, *Rev. Mod. Phys.* **66**, 1125 (1994).
- ²⁷ M. Putti, I. Pallecchi, E. Bellingeri, M. R. Cimberle, M. Tropeano, C. Ferdeghini, A. Palenzona, C. Tarantini, A. Yamamoto, J. Jiang, J. Jaroszynski, F. Kametani, D. Abaimov, A. Polyanskii, J. D. Weiss, E. E. Hellstrom, A. Gurevich, D. C. Larbalestier, R. Jin, B. C. Sales, A. S. Sefat, M. A. McGuire, D. Mandrus, P. Cheng, Y. Jia, H. H. Wen, S. Lee, and C. B. Eom, *Supercond. Sci. Technol.* **23**, 034003 (2010).
- ²⁸ A. Gurevich, *Annu. Rev. Cond. Matt. Phys.* **5**, 35 (2014).
- ²⁹ G. P. Mikitik and E. H. Brandt, *Phys. Rev. B* **68**, 054509 (2003).